A comparative study on the phase behaviour of highly charged colloidal spheres in a confining wedge geometry

Ana Barreira Fontecha[1]**, Hans Joachim Schöpe**[1]**, Hans König**[1]**,
Thomas Palberg**[1]**, René Messina**[2] **and Hartmut Löwen**[2]

[1] Institut für Physik, Johannes Gutenberg Universität Mainz, Staudinger Weg 7, 55128 Mainz, Germany
[2] Institut für Theoretische Physik II, Heinrich-Heine-Universität Düsseldorf, Universitätsstrasse 1, D-40225 Düsseldorf, Germany

Abstract
We studied the structures formed in aqueous dispersions of charged colloidal spheres under a constant low salt concentration of $c = 6 \times 10^{-6}$ mol l^{-1}. Particles of diameter $2a = 1000$ nm were confined to a low angle wedge geometry with plate separation $0 < S < 50$ μm and observed with video microscopy. Irrespective of the initial particle density n we reproducibly observe the particles to migrate to the narrow wedge side on the timescale of a few days. Thereby an interface between a crystalline structure and a near particle free region is formed, which propagates slowly until the dilute region is exhausted of particles. While the origin of this separation is still unclear, the final extension of the crystalline region is stable on the timescale of months. Within the crystal phase we observe a characteristic sequence of structures with increasing plate separation similar to that seen in previous experiments on hard sphere-like systems but here with non-touching particles. Moreover, we find that mechanical equilibrium is a necessary prerequisite for observing the full richness of different phases. A detailed comparison to recent theoretical calculations for bilayers was performed and semi-quantitative agreement with the predictions observed.

1. Introduction

It is well known from atomic matter studies that confinement may significantly alter the phase behaviour of materials [1]. This has also been seen in colloidal systems and a rich variety of structures were reported for slit or wedge confinement, which can partly be derived from the corresponding bulk structures. For example, buckled, triangular, rectangular, differently staggered rhomboedric and prism phases were reported for systems showing face or body

centred cubic structures (fcc, bcc respectively) in the bulk [2–9]. Experimental work was mainly performed for charged particles at (often not precisely defined) moderate to large salt concentration. Nevertheless under these circumstances the interaction is conveniently tuned between the theoretical limits of hard spheres and the one-component plasma, and in order to calculate phase diagrams it can be described using a pairwise additive screened Coulomb potential [10, 11]. Early theoretical work on the phase behaviour in confinement had addressed hard sphere particles [5]. Only recently was the bilayer phase behaviour calculated explicitly considering arbitrary screening lengths and particle densities [12]. The predictions were made also for weakly screened low density systems, which in the bulk would order in bcc structures.

To test these predictions experimentally, in principle extensive density and plate separation dependent measurements are required at reproducibly adjusted low electrolyte concentrations. To check the latter point we decided to work at carbonate saturated conditions but in otherwise salt free conditions. Further, samples of different initial density were used in wedge cells of laterally varying height. For this contribution we focus on one initial density; the results for all other initial densities are practically the same. The rest of the paper is organized as follows. We first give experimental details of sample preparation and cell construction. We then discuss the migration phenomenon observed in some detail. Structure analysis is then performed on the stable crystalline structures in the narrow part of the wedge and a comparison to previous experiments and the theoretically expected bilayer behaviour is given.

2. Experimental details

We used commercially available polystyrene spheres of diameter $2a = 1000$ nm with a size polydispersity smaller than 3%. The effective charge from conductivity used for later calculations was $Z^* = (6860 \pm 150)$. A stock suspension was prepared in contact with ion exchange resin at a particle density of $n \approx 20 \ \mu\text{m}^{-3}$. From this the desired densities were adjusted by dilution with distilled water. Samples were left in contact with air to obtain saturation with air-borne carbonate. The saturation process is conveniently and accurately monitored by means of the conductivity [13]. More importantly it is quite well reproducible, if performed at constant temperature. Consistently with the literature [14], control measurements yielded $c = (6 \pm 1) \ \mu\text{mol} \ \text{l}^{-1}$ at $T = (295 \pm 2)$ K over a wide range of initial particle densities and for different particle species. The major contribution to the screening of the electrostatic repulsion, however, stems from the particle counter-ions. The screening parameter is calculated via $\kappa^2 = e^2/(k_\text{B}T\epsilon_0\epsilon_\text{r}) \sum_i n_i z_i^2$, where e is the elementary charge, $k_\text{B}T$ is the thermal energy and $\epsilon_0\epsilon_\text{r}$ is the dielectric permittivity of the solvent with $\epsilon_\text{r} = 80$ for water. n_i is the number density and $z_i = 1$ the valency of the micro-ions of species i.

Wedge cells were constructed from standard microscopy slides of 1 mm thickness and lateral dimensions of $(X \times Y) = (25 \times 75) \ \text{mm}^2$. Prior to use these were cleaned with acetone and rinsed with distilled water and dried in a dust free stream of Ar. At one end an $(8 \times 2) \ \text{mm}^2$ piece of 50 μm polycarbonate foil was placed between two slides to result in a wedge of small angle $\alpha = 0.04°$. The cell was sealed at its rim with perfluorinated, water insoluble vacuum grease (Glisseal, Bohrer, CH), with two tiny openings left at the ends of the cell. The suspension was then brought into contact with one of these openings and sucked in by capillary forces. In this way bubble free samples were conveniently obtained. The cell was then completely sealed and mounted on the stage of an inverse microscope for observation. We used Köhler illumination with white light and a 63× long distance high resolution objective (PL Fluotar L 63×/0.7 corr PH2 ∞/0.1−1.3/C; working distance 1800 μm, Leitz, Germany). Images were recorded with a black and white SVHS CCD camera (EHDcamPro04*, EHD Physikalische Technik, Germany) and stored in a computer for later evaluation. The objective focal plane

can be moved through the sample by a piezo-electric drive (PI, Germany). This allowed for a check of the geometry with an accuracy of ± 300 nm. We found that in most cases the increase in S in the slope direction was linear with X. In the perpendicular Y-direction the plates were not completely parallel to each other. In fact, the mid-cell region was often found to be less narrow than the rim region. Use of the piezo-drive also allowed measurements of the interlayer distances D in the crystalline parts of the sample. For comparison to the theoretical predictions, this and the locally determined screening parameter determine one of the relevant quantities: $\lambda = \kappa D$. The other one is the reduced areal density, $\eta = \rho D^2/N$, which is derived from the areal density ρ of the X–Y projection of the recorded images and the layer number N.

Just after filling the cell we observed a homogeneous particle density throughout the sample. For a given volume at the wide side of the wedge we performed particle counts to check the particle number density and found good agreement with the values obtained during preparation from conductivity. On the timescale of several hours, however, particles were reproducibly observed to migrate towards the narrow part of the wedge. In this way a concentrated region was formed there and a depleted region was formed in the remaining part with a gradient in particle density. The concentrated region was usually separated from the depleted region by a rather sharp interface. A typical situation is shown in figure 1. In the concentrated region crystalline structures were formed. We observe a slight compression occurring in the crystalline region after crystallization leading to a rearrangement of crystal structures. Note in figure 1 that the crystals start with a square structure which in the course of time changes to rhomboedric and finally triangular. The triangular structure was then observed to be stable at this cell position. The crystals were separated from the depleted region by a thin quasi-liquid layer. The position of the interface advanced at velocities of a few microns per hour. It usually slowed after some weeks to leave a stable situation of a crystalline region in the narrow part and a practically particle free region in the remaining cell. The final position of the interface was observed to depend on the initial particle density. The larger the initial n, the further the interface had advanced before particle exhaustion. In this way stable interfaces at different layer numbers were prepared. Below we concentrate on the results for $n = 4 \times 10^{18}$ μm^{-3}, where the interface was observed for a five-layer state.

The origin of this effect remains hidden. We carefully checked several possible experimental artefacts, like contamination by a local source of electrolyte, evaporation, gradients of temperature or of solvent composition, and gravity, which we believe can all be excluded. Unusual behaviour in charged sphere systems has been observed before. It has been discussed in connection to the possibility of like charge attraction occurring in the vicinity of charged walls. This discussion, however, is still open both experimentally and theoretically [15, 16]. Since the main interest of our contribution is not affected by that point, we refrain from further speculation. More importantly, practically all samples investigated showed this behaviour and the interfacial position remained stable over extended periods of time (for the sample discussed below, now for more than six months). We therefore simply state that we are able to reproducibly prepare stable multilayer crystalline systems with well defined salt concentrations and resulting particle densities.

3. Results

Overall inspection of the samples showed the well known principal sequence of phases going from $N\triangle$ to $(N+1)\square$ to $(N+1)\triangle$, where N denotes the layer number and $\triangle$ and $\square$ a triangular and square, respectively, symmetry. Here we follow the notation originally introduced by Pieranski and later extended by Neser *et al* [2, 4]. Like in previous experimental studies on
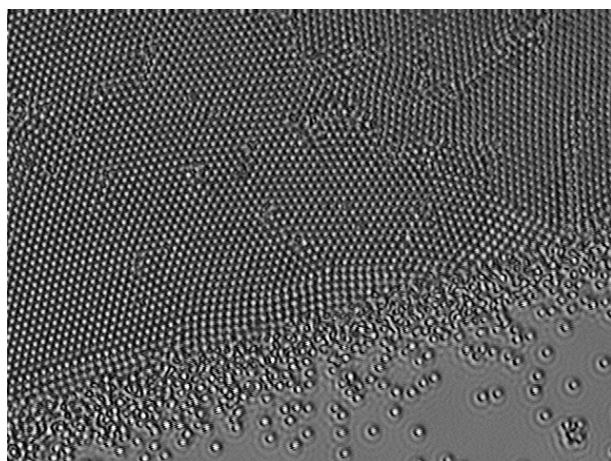
Figure 1. Advancing interface between the narrow wedge region (top) filled with crystalline ordered particles and the wider region depleted of particles (bottom) (image width (70.7×53.0) μm^2). The origin of this well reproducible effect is not yet known. The interface advances at speeds of some microns per hour until the complete remaining cell is void of particles. It comprises a thin quasi-liquid layer of short ranged order but elevated density. The crystalline region gets slightly more concentrated over time and shows a gradual transition between different structures ($2\square \rightarrow 2Ra \rightarrow 2\triangle$).

nearly hard spheres [4, 17] these phases were observed to be separated by intermediate regions of prism structure with prisms of quadratic or triangular symmetry of their base plane, denoted as $NP\square$ and $NP\triangle$, respectively, with N here giving the width of the prism base. In our case of low growth velocities in the crystalline region these prism phase regions are much larger than under strong lateral solvent current [4, 17] and nearly as extended as the square and triangular regions. With increased cell height the prisms are shifted vertically with respect to each other, optimizing the packing efficiency [4]. The packing density may also be enhanced by other buckling-like reconstructions and by the use of differently sized prisms. In contrast to the hard sphere case, in our experiments the particles are not at close contact; rather they are separated with an interparticle distance of $d = 2.2a$, where a is the particle radius. This circumstance may favour the occurrence of different sometimes degenerate prism phases. For the $N = 1$ to 2 transition the situation is even more complicated, as now also a buckled phase B and two rhomboedric phases, $2Ra$ and $2Rb$, may appear. The buckled phase appears as particles assorted in rows of alternating vertical position [6]. The rhomboedric phases display two different stackings with a central interdigitation ($2Ra$) and an off-centre digitation ($2Rb$). A set of images documenting the experimentally observed bilayer phases is given in figure 2.

The complete observed sequence for our case of charged spheres close to mechanical equilibrium was the following:

$$
\begin{aligned}
&1\triangle \rightarrow B \rightarrow 2\square \rightarrow 2Ra \rightarrow \\
&2\triangle \rightarrow (2P\square + 2P\triangle) \rightarrow 3\square \rightarrow (3Ra + 3P\square + 3P\triangle) \rightarrow \\
&3\triangle \rightarrow 3P\square, \rightarrow 4\square \rightarrow (4P\square + 4P\triangle) \rightarrow \\
&4\triangle \rightarrow (4P^* + 4H^*) \rightarrow 5\square \rightarrow 5P^* \rightarrow 5\triangle.
\end{aligned}
\tag{1}
$$

At certain separations we find the simultaneous occurrence of different prism phases with base width equal to the layer number N of the preceding stable square or triangular phase. At larger S also complicated packings of prisms with base widths smaller than N
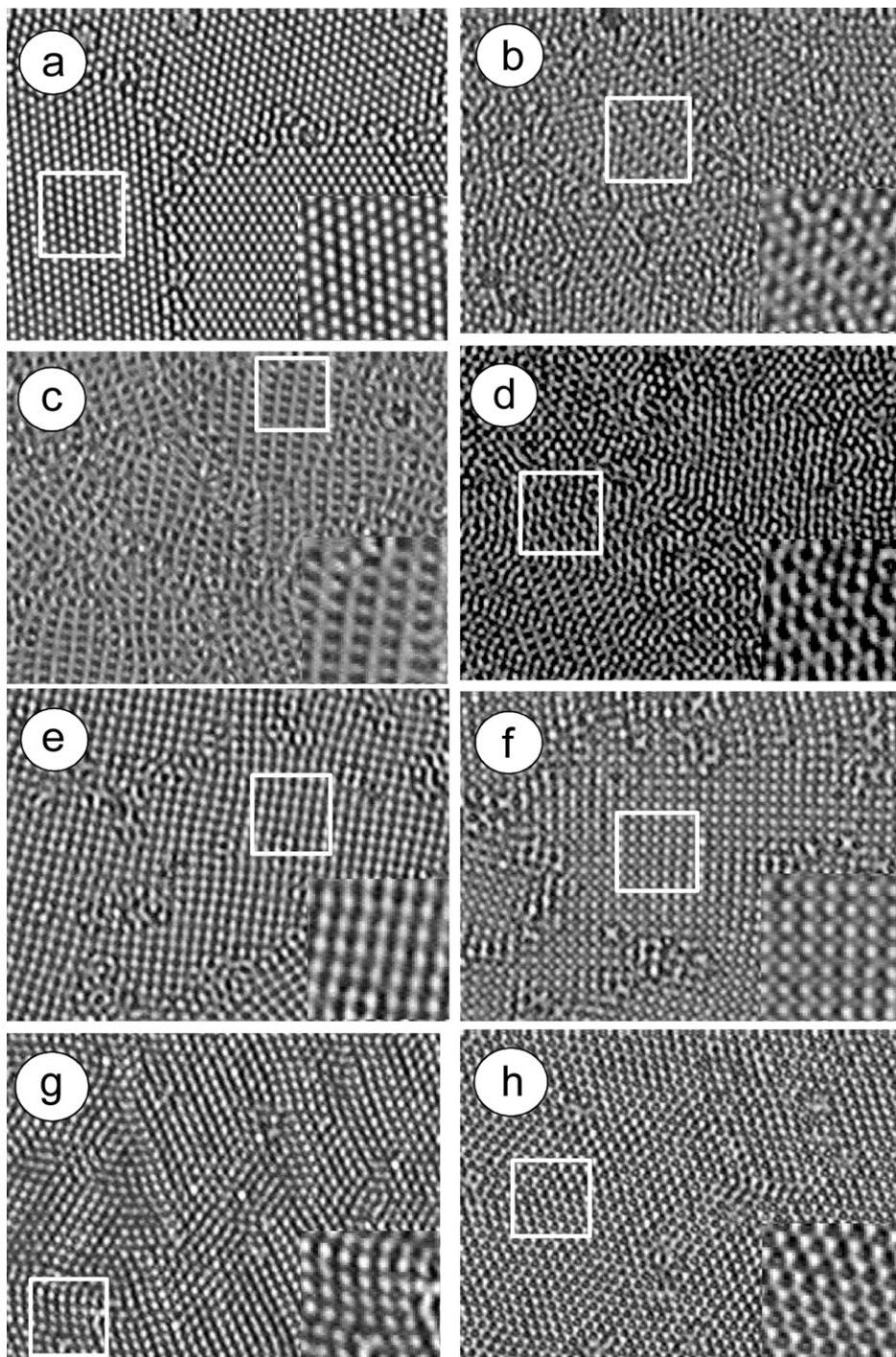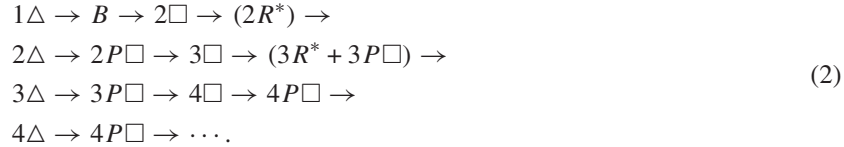
Figure 2. Images of structures taken for the equilibrated sample at the transition from a monolayer to a bilayer; image width (47.2×35.4) μm^2. The white squares indicate the position of the fourfold enlargements shown bottom right in the images. We observe the following structures with increased plate separation: (a) $1\triangle$; (b)–(d) B; (e) and (f) $2\square$; (g) $2Ra$; (h) $2\triangle$.

were observed, as well as aesthetically very pleasing rosette-like reconstructions of hexagonal symmetry (H^*). Both types of not yet fully characterized structure are denoted with an asterisk. The reported sequence is similar to that observed by Neser in still dispersed effective hard sphere suspensions at elevated salt concentrations after crystallizing at interfacial velocities of the order of 0.5 μm h^{-1}. In particular, there a $2R^*$ and a $3R^*$ phase were observed first [17]. This is, however, different to the sequence expected from the purely geometrical hard sphere model, where for each separation only a single structure should exist and the degeneracy observed here is not expected [2, 4].

For the case of charged spheres completely dried from suspensions at elevated salt concentration the following sequence has been reported [17]:

$$
\begin{aligned}
1\triangle &\rightarrow B \rightarrow 2\square \rightarrow (2R^*) \rightarrow \\
2\triangle &\rightarrow 2P\square \rightarrow 3\square \rightarrow (3R^* + 3P\square) \rightarrow \\
3\triangle &\rightarrow 3P\square \rightarrow 4\square \rightarrow 4P\square \rightarrow \\
4\triangle &\rightarrow 4P\square \rightarrow \cdots.
\end{aligned}
\tag{2}
$$

We note a general close agreement, but also some specific differences. In particular, the completely dried sample does not show the full richness of possible prism phases. Their occurrence can be further reduced by performing a very fast drying process from a drop placed on a single flat surface. For that experiment very often the following sequence is observed [18]:

$$
1\triangle \rightarrow 2\square \rightarrow 2\triangle \rightarrow 3\square \rightarrow 3\triangle \rightarrow 4\square \cdots.
\tag{3}
$$
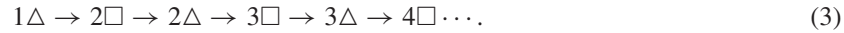
Here the rhomboedric and the prism phases are completely missing. From these comparisons two qualitative trends can be identified. First, for charged spheres, degeneracy between different prism phases seems to be the rule rather than the exception. This is corroborated by previous reports on charged spheres at low salt concentration confined to parallel plate slits. There additional degenerate phases were observed for small N [7]. Second, the presence of large lateral forces, e.g. capillary forces upon drying, drastically reduces the number of observable phases in the dry state. Buckled, rhomboedric and in particular the prism phases are laterally compressed to reach the next $N\square$ or $\triangle$ phase.

A more quantitative comparison to recent theoretical predictions is possible for the bilayer phase behaviour [12]. The stable crystalline phase for bilayer systems was calculated assuming a pairwise additive Yukawa interaction $\propto \exp(-\kappa r)/r$ between the particles and a small temperature. The phase behaviour found in [12] is very rich including two different rhomboedric phases and re-entrant behaviour for a varied range of the Yukawa interaction at fixed particle density. The phase diagram is conveniently expressed in terms of the reduced number density $\eta = \rho D^2/2$ of colloids per area and the inverse range $\lambda = \kappa D$ of the interaction, scaled with the layer separation distance D.

We next map the experimental parameters onto the theoretical phase diagram by assuming a Debye–Hückel inverse screening length $\kappa^2 = e^2/(k_B T \epsilon_0 \epsilon_r) \sum_i n_i z_i^2$. Here we explicitly include the contribution of particle counter-ions to the small ion densities n_i. Following earlier work [20], we express the counter-ion density as $n_i = n Z^*$ where Z^* is the effective charge of the particles and n is the local particle number density for each given phase. The sum then reads: $\sum_i n_i z_i^2 = n Z^* + 2 \times 1000 N_A c$, where N_A is the Avogadro number and c is the concentration of background electrolyte. Note that contributions of the cell wall counter-ions to the screening are neglected in this approach which may lead to a slight underestimation of κ. The particle number density is measured locally by microscopy. As an example, for the buckled phase B one obtains $n = 2/(a \times b \times D)$, where a and b refer to the side lengths of the unit cells used in the bilayer plasma notation [12, 19]. This notation is also adopted in figure 3. Here region I corresponds to $1\triangle$, region II to B, region III to $2\square$, regions IVa and IVb to $2Ra$
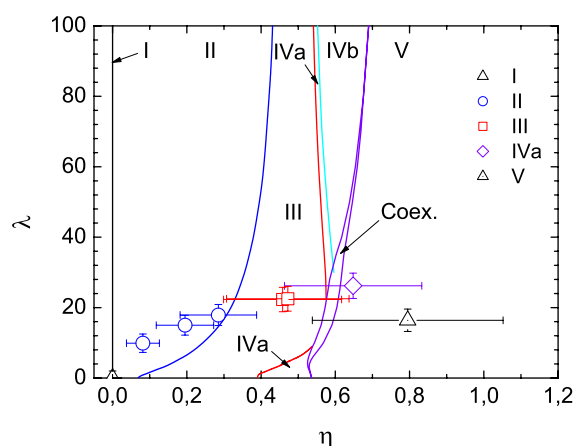
Figure 3. Comparison of the theoretical prediction for the bilayer phase diagram to the experimental data corresponding to the images shown in figure 2. Data are plotted in the $\eta = \rho D^2/2$–$\lambda = \kappa D$ plane. Symbols denote the positions of the experimentally observed phases. Solid lines correspond to the theoretical phase boundaries between the phases indicated in plasma bilayer notation [19]. Despite the large error bars stemming from the uncertainties of our distance measurements, a semi-quantitative overall agreement is observed. A coexistence region is marked by 'Coex'. For details see the text.

(This figure is in colour only in the electronic version)

and $2Rb$, respectively, and region V to $2\triangle$. In figure 3 the locations of the phases shown in figure 2 are compared to our theoretical expectations. Due to the experimental uncertainty in a, b and the layer separation distance D, there is an error bar on the two quantities η and λ. The propagation of the uncertainties in the former quantities to η is more severe than that to λ. Despite the large error in η there is good agreement both in the qualitative sequence of the different phases and in the actual locations of the different crystal structures. As expected, for charged spheres we observe the centred rhomboedric phase IVa instead of IVb. The positions of the buckled the $2\square$ and the triangular phases are in good agreement with the theoretical predictions. Only region IVa is slightly off prediction. We note that the inclusion of wall counter-ions would shift our experimental data upward leading to an even better agreement.

4. Concluding remarks

In conclusion we have presented experimental evidence that different sequences of crystalline structures occur in confined charged suspensions, if (i) the salt concentration is altered to move from the hard sphere limit to a situation of longer ranged repulsion and (ii) the sample is not dried completely but rather is prepared in suspension close to mechanical equilibrium. In the bilayer regime, semi-quantitative agreement with theoretical calculations was achieved as far as both the qualitative sequence and the quantitative numbers are concerned. In future, further quantitative investigations are needed. First, theoretical investigations for larger layer numbers $N > 2$ are needed. Second, with the use of differently sized particles, different (in particular lower) values of λ would become accessible. This allows one to test the theoretically predicted re-entrant behaviour. Finally one should perform a finer experimental scan through the whole parameter space with precise determination of the positions of the phase boundaries. In the present study using a wedge geometry this was hindered by the occurrence of the phase

separation-like phenomenon shown in figure 1. Here also more work is needed, as its origin remains unexplained at the present stage.

Acknowledgments

References

[1] Binder K 1998 *J. Non-Equilib. Thermodyn.* **23** 1
[2] Pieranski P, Strzlecki L and Pansu B 1983 *Phys. Rev. Lett.* **50** 900
[3] van Winkle D H and Murray C A 1986 *Phys. Rev.* A **34** 562
[4] Neser S, Bechinger C, Leiderer P and Palberg T 1997 *Phys. Rev. Lett.* **79** 2348
[5] Schmidt M and Löwen H 1996 *Phys. Rev. Lett.* **76** 4552
    Schmidt M and Löwen H 1997 *Phys. Rev.* E **55** 7228
[6] Neser S, Leiderer P and Palberg T 1997 *Prog. Colloid Polym. Sci.* **102** 194
[7] Murray C A 1998 *MRS Bull.* **23** 33
[8] Murray C A, Sprenger W O and Wenk R A 1990 *Phys. Rev.* B **42** 688
[9] Bechinger C 2002 *Curr. Opin. Colloid Interface Sci.* **7** 204
[10] Robbins M O, Kremer K and Grest G S 1988 *J. Chem. Phys.* **88** 3286
[11] Voegtli L P and Zukoski C F IV 1991 *J. Colloid Interface Sci.* **141** 79
[12] Messina R and Löwen H 2003 *Phys. Rev. Lett.* **91** 146101
[13] Wette P, Schöpe H-J, Biehl R and Palberg T 2001 *J. Chem. Phys.* **114** 7556
[14] Millero F J 1995 *Geochim. Cosmochim. Acta* **59** 661
[15] Grier D G and Han Y 2004 *J. Phys.: Condens. Matter* **16** S4145
[16] It is worth noting that the experimental parameters here are rather comparable to those of Larsen A E and
     Grier D G 1996 *Phys. Rev. Lett.* **76** 3862 who observed a similar phenomenon
[17] Neser S 1999 *PhD Thesis* Konstanz
[18] Evers M 2000 *PhD Thesis* Mainz
[19] Goldoni G and Peeters F M 1996 *Phys. Rev.* B **53** 4591
[20] Wette P, Schöpe H J and Palberg T 2002 *J. Chem. Phys.* **116** 10981